Dust Destruction and Ion Formation in the Inner Solar System

Ingrid Mann

Institut für Planetologie, Westfälische Wilhelms-Universität, Münster, Germany

imann@uni-muenster.de

and

Andrzej Czechowski

Space Research Center, Polish Academy of Sciences, Warsaw, Poland

ace@cbk.waw.pl

ABSTRACT

We suggest that dust-dust collisions feed ions into the interplanetary medium and produce a significant amount of the inner source heavy pick-up ions detected by the Solar Wind Ion Composition Spectrometer (SWICS) aboard the Ulysses spacecraft. Organic refractory material contained in the cometary dust could explain the existence of carbon among the measured pick-up ions. Impact-produced ions may locally influence the plasma parameters of the solar wind. It will be possible to study in-situ these dust-plasma interactions and the central region of meteoroid activity through measurements in the inner solar system proposed for the currently discussed Solar Probe and Solar Orbiter missions.

Subject headings: solar wind — interplanetary medium – meteoroids

1. Introduction

In the inner region of the heliosphere (less than about 1 AU from the Sun) numerous small interplanetary bodies, from dust grains to comets, meet their demise. Dust orbital motion combines with Poynting-Robertson deceleration to increase the dust number densities towards the Sun. Collisional fragmentation causes the average mass of bodies to decrease. To maintain the dust mass distribution, this collisional net loss must be compensated for by supply of larger grains, and it is likely that fragmentation of cometary meteoroids feeds the dust cloud inward from 1 AU (Grün et al. 1985; Ishimoto 2000; Mann et al. 2004). We

propose that during this process a significant amount of dust material is released into the interplanetary medium by vaporization and sublimation.

The released gas and the ions should contribute to the heavy component of the inner source pick-up ions (Geiss et al. 1996). Pick-up ions differ from the bulk solar wind by their charge state and velocity distribution. They are released from solar system objects or generated through ionization of neutrals such as the interstellar gas that enters the solar system (Gloeckler & Geiss 2001). The Solar Wind Ion Composition Spectrometer (SWICS) aboard the Ulysses spacecraft discovered the pick-up ions from an inner source localized near the Sun and the spatial distribution of the source suggests it may originate from dust destruction or dust surface interactions (Geiss et al. 1996; Gloeckler & Geiss 1998; Schwadron et al. 2000). Interestingly, the published fluxes for the heavy inner source pick-up ions: 2 10^3 kg/s for oxygen and carbon each (Geiss et al. 1996) are consistent with the earlier estimations (9 10^3 kg/s) of the dust mass loss in the interplanetary dust cloud within 1 AU from the Sun (Grün et al. 1985).

To estimate how dust collisions contribute to the inner source of the pick up ions we calculate the ion production by dust collisions and compare it to other dust-related ion production processes (section 2). We calculate the charge states of the generated ions at 1 AU (section 3) and discuss the element abundances of the collision-produced pick-up ions as well as their implications for the inner solar system dust cloud (section 4). In section 5 we summarize our results and discuss them with regards to past and future space measurements.

2. Ion Production from Dust

From analytical theory and numerical simulations describing the propagation of impact induced shock waves in solids one can estimate the amount of fragments and vapor produced by mutual collisions of dust grains. We use the formulae previously applied to the evolution of dust in the interstellar medium (Tielens et al. 1994; Jones et al. 1996) for the model parameters of silicate, carbon and ice. A slightly simplified description of our collision model follows. The vaporized (fragmented) parts of the target mass m_1 are proportional to the projectile mass m_2, with the coefficients c_{vap} (c_{frag}) depending on the relative velocity v and on the material of colliding grains: $c_{vap} = c_{vap,0}(v/(5000m/s))^{\gamma}$, $\gamma \approx 1.75$, and similarly for c_{frag}. The distribution of fragments is of the form $m^{-\eta}$, $\eta = 0.76$, with the largest fragment mass, m_L, determined as $m_L/m_1 = (0.2\ v_{cat}/v)^3$, where $v_{cat} = const\ (m_1/m_2)^{9/16}$ is the critical fragmentation velocity. If $m_1 \leq c_{vap}\ m_2$, the whole target is vaporized. For the cases of carbon, ice and silicate grains we assume respectively $c_{vap,0} = (0.301, 7.39, 0.343)$, $c_{frag,0} = (60.5, 29.3, 14.5)$, and $v_{cat} = (7.8\ 10^4\ m/s, 1.2\ 10^5\ m/s, 1.83\ 10^5\ m/s)$, the latter for

the case of 5 nm projectile and 100 nm target. Due to short sublimation lifetimes we don't expect a permanent cloud of icy grains in the inner solar system, but we include ice as an example of a material with high efficiency of the impact vaporization. Grains are assumed to be spherical and homogeneous. We note that for irregularly shaped porous particles, both the ion production by collisional vaporization and by the surface interaction (see below) increase.

We assume the following model of the dust cloud inside 1 AU: The mass distribution is independent of the heliocentric distance and given by either the interplanetary flux model (IFM) (Grün et al. 1985) or by its modification obtained by changing parameters in the IFM formula: $c_5 \rightarrow 0.7c_5$, $c_7 \rightarrow 1.0\ 10^{-4}c_7$, $c_8 \rightarrow 3.0\ 10^{10}c_8$. The modified distribution has the density enhanced by up to a factor of 3 in the middle mass range and agrees with some recent measurements (Love & Brownlee 1993). We assume a lower cutoff in mass at 10^{-21} kg, because smaller grains would be removed by the Lorentz force.

The radial dependence is of the power-law form $r^{-\chi}$ outside 10 solar radii (R_{Sun}) and flat inside 10 R_{Sun}, with the inner cut-off at $r = 2\ R_{Sun}$. We consider two cases of the latitudinal distribution: 'one-component', concentrated near the ecliptic plane (which takes 23% of the volume of the sphere) with $\chi = 1.3$, and the 'two-component' model consisting of the ecliptic component with $\chi = 1$, and a spherical component with a steeper increase toward the Sun ($\chi = 2.0$). In the two-component model, the ecliptic component is taken to amount to 90% of the total grain density at 1 AU. Both models are consistent with zodiacal light observations and with our understanding that comets and asteroids are the main sources of the dust cloud (Mann et al. 2004). The average relative velocities v_0 of the grains at 1 AU are assumed to be $2\ 10^4$ m/s if both grains belong to the ecliptic component, $3\ 10^4$ m/s if both belong to the spherical component and $4\ 10^4$ m/s if they belong to different components. In all cases the relative velocity behaves as $v(r) = v_0\ r^{-0.5}$. We label the models as follows: (A) IFM, one-component; (B) one-component using the modified flux distribution; (C) IFM, two-component; and (D) two-component using the modified flux distribution. We consider the model (C) to be probably the most plausible case since it combines the spherical component suggested by some observations (Mann et al. 2004) with the widely accepted mass distribution at 1 AU (IFM).

Figure 1 illustrates the mass balance for the model (A) at 0.3 AU. The loss rate of the mass m grains (by fragmentation and vaporization) and the production rate of fragments of mass m are presented as a function of m. For comparison, we show by the thin lines the results of Grün et al. (1985), which correspond to the same grain distribution but a different fragmentation model (not including vaporization). Our collision model is more conservative as it corresponds to a smaller fragmentation rate. Note that, in our model, vaporization is

the dominant destruction mechanism of small grains.

Similarly to the previous studies we find the net mass gain to be negative for large mass and positive for low mass region (Figure 1) with the dividing mass at 10^{-10} to 10^{-9} kg (Grün et al. 1985; Ishimoto 2000). The net mass gain integrated over the low mass range provides an estimate of the mass supply needed to maintain the mass distribution. The results from model calculations are presented in Table 1. We find almost equal ion production from the near ecliptic and the remaining region: since the ecliptic region constitutes only 23% of the volume, this means that the pick-up ion flux is enhanced near the ecliptic.

As an example, the radial source distribution of oxygen assuming it is produced by collisional vaporization of SiO_2 grains is shown in the Figure 2, which also presents the results for the solar wind desorption mechanism. This mechanism is based on the observation that solar wind ions are implanted in the surface layer of dust grains and reach saturation on time scales short compared to the dust lifetime. The impact of additional solar wind ions is balanced by release of the neutral atoms, which was suggested to produce neutral hydrogen and helium near the Sun (Fahr et al. 1981). To obtain pick-up ion fluxes compatible with the observed inner source flux assuming the desorption mechanism requires a very large dust number density. This is illustrated in Figure 2, with the curve (F) showing the source distribution required to produce the observed flux of oxygen ions and the curve (E) showing the result for our model (A). Production of ions from solar wind desorption within 1 AU is ($1.4\ 10^2$, $4.5\ 10^2$, $4.0\ 10^2$, $1.2\ 10^3$) kg/s for the models (A), (B), (C) and (D), respectively, with the ion content of the solar wind (mostly hydrogen, with only a small fraction in the heavy species).

Solar wind ions will pass through grains whose sizes are smaller than the penetration depth of solar wind particles with an energy loss proportional to their path length (Minato et al. 2004) and will then acquire single or neutral charge state. This was suggested as a possible mechanism to produce inner source pick-up ions (Wimmer-Schweingruber & Bochsler 2003). For the dust distribution models considered above, ion production from the passage of solar wind particles through grains is below that of the solar wind desorption and below ion production by collisions. Assuming an enhanced amount of small grains would increase ion production from this mechanism, but would also increase collision rates and therefore collisional vaporization. Dust sublimation occurs mostly inward from about 0.05 AU (Mann et al. 2004) and is not studied here in detail, since it produces predominantly multiple charged ions (see below).

3. Charge States of Ions

The production of vapor from the grains increases near the Sun and we need to consider the possibility of higher ionization states of the heavy species. Numerical simulations of impact vaporization suggest the produced vapor has a temperature of the order of 10^4 K to 10^5 K and consists mainly of neutral and singly charged species (Hornung & Kissel 1994). The ion thermal speed is thus less than the grain orbital speed and we may assume that the release of the atom from the grain and its first ionization take place at the same distance from the Sun. The main ionization mechanisms are: photoionization, charge exchange with the solar wind protons, and electron impact ionization close to the Sun. Time scales for ionization of the neutral oxygen or carbon atom due to the first two mechanisms are of the order of 10^6 s -10^7 s at 1 AU (i.e. less than an orbital period) and decrease rapidly toward the Sun. Singly ionized species are picked up within the Larmor rotation time of the order of seconds.

To estimate the distribution of charge states of the inner source pick-up ions arriving at 1 AU we solve the evolution equations for the oxygen and carbon ions, taking into account photoionization and electron impact ionization for selected models of the solar wind. We use the fits for the electron-impact ionization rates (Arnaud & Rothenflug 1985), the photoionization cross sections (Verner et al. 1996), the radiative and dielectronic recombination rates (Shull & van Steenberg 1982) and the charge-exchange cross sections (Phaneuf et al. 1987). We don't include the ionization by solar wind protons. Since omitting one of the ionization processes should tend to lower the final ionization state, the fraction of higher ionization states calculated in our approach may be underestimated. The solar wind models are defined in terms of the electron temperature and the velocity profiles, assuming radial expansion for simplicity. For the slow solar wind we use a model based on electron temperatures derived from Helios measurements (Marsch et al. 1989) and the velocity profile for a slow stream derived from coronagraph observations (Sheeley et al. 1997). For the fast solar wind we use the Cranmer (2002) model.

In Figure 2 we show the effective radial source distributions of the oxygen ions that arrive at 1 AU in the single-charge state (dashed curves) for each of our 4 models. These are obtained by folding the radial source distributions with the calculated probability of the ion reaching 1 AU singly-charged. Our results for charge state distributions of the oxygen and carbon ions at 1 AU are shown in Figure 3. The abundance of the different charge states depends on the distance from the Sun where the ions are released (Figure 3) and on the species ionisation rates. For ions generated inward from 0.1 AU multiple charge states are abundant which may explain the inner cut-off of the inner source seen in the SWICS data. Ionization varies with the solar wind speed and is less effective in the polar region of

fast solar wind where the cut-off for singly charged ions moves further inward. We find that about 75% of carbon is singly charged compared to 56% for the slow solar wind case. The amount of singly charged oxygen increases from 49% in the slow solar wind to 65% in the fast solar wind. This may explain some of the differences in the source distributions derived from experimental data (Gloeckler et al. 2000a; Schwadron et al. 2000).

4. Element Abundances

Ions produced by impact vaporization have roughly the elemental composition of the dust and meteoroids. Nevertheless, the abundances of observed singly charged ions are influenced by variation of the ionization rates with the species and with solar wind parameters. The inner source pick-up ions are at present identified for the elements H, C, N, O, Mg (and/or mass 24 molecules), Si (and/or mass 28 molecules), and Ne with abundances that are similar to the solar wind (Gloeckler & Geiss 2001). While the detection of carbon was previously assumed to rule out the direct supply of meteoritic material as the major source (Geiss et al. 1996), its origin may also be cometary dust and meteoroids that locally produce a significant part of the dust cloud inward from 1 AU (Mann et al. 2004). Cometary material is more pristine and its composition closer (but not identical) to solar abundances than the common meteoritic composition. Indeed a high content of the elements C, H, O, N compared to meteoritic abundances was measured in-situ for dust at comet Halley with about the same amount of C and O (Jessberger et al. 1988). If our model of the inner source is correct, then the presence of carbon in the inner source indicates that cometary dust contains carbon in the form of organic refractory material that can survive high temperatures in the inner solar system. Cometary meteoroids may also contain volatiles implanted in the minerals as recently indicated by the possible detection of a hydrogen emission line in the Leonid meteor trails (Pellinen-Wannberg et al. 2004). Since most remote sensing observations in cometary dust tails are of ionized species, little is known about the amount of noble gases from cometary dust and meteoroids. They may be present to some degree, since observations of comet Hale-Bopp, for instance, are interpreted assuming that the comet contains more than 15% - 40% of largely unprocessed interstellar material (Blake et al. 1999). On the other, hand in-situ composition measurements in cometary ion tails (Gloeckler et al. 2000b) indicate N and particular Ne abundances far below solar values. Solar wind particles implanted in the surface of the dust grains are a source of noble gases and light elements. All these findings make it plausible that the ions produced by impact vaporization contain light elements and noble gases, but not to the same amount as in the solar wind. If the composition of inner source pick-up ions is indeed the same is that of the solar wind, then vaporization due to dust-dust collisions alone is unlikely to be the dominant source of these

pick-up ions. While light elements (primarily C and O) are also directly supplied by comets (Gloeckler et al. 2000b), we expect that for a continuous ion production the direct supply from comets to be less important since for the case of the frequently occurring sun grazing comets the mass supply to the solar vicinity amounts to 2 10^2 kg/s (Mann et al. 2004).

5. Discussion

In summary, our calculations show that collisional vaporization can produce the heavy pick-up ion fluxes of the inner source. Our estimation is likely to be low since laboratory measurements show a higher degree of impact ionization for low impact velocities (Hornung & Kissel 1994). Moreover, part of the dust production may occur in spatially concentrated meteoroid trails (Mann et al. 2004). This increases the ion production from collisional vaporization and in certain cases also from solar wind desorption. The solar wind desorption mechanism is not efficient enough to explain the observed inner-source hydrogen flux of 4 10^4 kg/s (Geiss et al. 1996) for any of the four dust models used here. Assuming higher dust number densities, in particular of small grains, furthermore increases the ion production by collisional vaporization compared to the solar wind desorption by dust grains.

The current models may miss a part of the dust-plasma interactions that take place near the sun since knowledge of both, collisional vaporization and solar wind surface interactions is mainly based on theoretical considerations. Measurements of the inner solar system dust cloud are limited and high velocity collisions can not be studied under laboratory conditions.

The collisional production of ions in the interplanetary medium is, however, detected for dust impacts on spacecraft. These produce electrons, protons and heavy ions and are known to influence plasma and magnetic field measurements as observed recently during encounter of DS1 at comet Borelli (Tsurutani et al. 2004). Similar to the comet Borelli events collisional evaporation, especially when taking place in cometary meteoroid trails, can be expected to influence the solar wind parameters measured locally from spacecraft. This is in agreement with observations of interplanetary field enhancements over time spans from minutes to hours that are possibly caused by mass loading of the solar wind plasma (Jones et al. 2003). The events occur clustered in space, more frequently in the inner solar system. The interplanetary field enhancements measured with Ulysses are correlated with solar wind crossing meteoroid trails (Jones et al. 2003). They possibly result from mass loading of the solar wind plasma induced by collisional vaporization in the dust trails. We expect this effect will be observed more frequently and can be studied more closely with in-situ measurements in the vicinity of the Sun. Measurements of collisional vaporization and dust plasma interactions should therefore be considered in planning of future space missions

such as Solar Orbiter and Solar Probe (Marsch et al. 2002; Möbius et al. 2000).

This research has been supported by the German Aerospace Center, DLR under the project 'Mikro-Impakte' (RD-RX-50 OO 0203). Part of this research was carried out during A.C.'s stay at the Institute of Planetology; his Guestlectureship was funded by Westfälische Wilhelms-Universität Münster. We thank George Gloeckler for his careful review of the manuscript.

REFERENCES

Arnaud, M., Rothenflug, R. 1985, Astron. Astrophys. Suppl., 60, 25

Blake, G. A., Qi, C., Hogerheijde, M. R., Gurwell, M. A., Muhleman, D. O. 1999, Nature 398, 213

Cranmer, S. R., 2002, Space Science Revs. 101, 229

Fahr, H. J., Ripken, H. W., Lay, G. 1981, Astron. Astrophys., 102, 359

Geiss, J., Gloeckler, G., von Steiger, R. 1996, Space Sci. Rev., 78, 43

Gloeckler, G., Geiss, J. 2001, Space Sci. Rev., 97, 169

Gloeckler, G., Fisk, L. A., Geiss, J., Schwadron, N. A., Zurbuchen, T. H. 2000a, J. Geophys. Res., 105, 7459

Gloeckler, G., et al. 2000b, Nature, 404, 576

Gloeckler, G., Geiss, J. 1998, Space Sci. Rev., 86, 127

Grün, E., Zook, H. A., Fechtig, H., Giese, R. H. 1985, Icarus, 62, 244

Hornung, K., Kissel, J. 1994, Astron. Astrophys., 291, 324

Ishimoto, H. 2000, Astron. Astrophys., 362, 1158

Jessberger, E. K., Christoforidis, A., Kissel, J. 1988, Nature, 332, 691

Jones, A. P., Tielens, A. G. G. M., Hollenbach, D. J. 1996, ApJ, 469, 740

Jones, G. H., Balogh, A. , McComas, D. J., MacDowall, R. J. 2003, Icarus, 166, 297

Love, S.G. & Brownlee, D. E. 1993, Science, 262, 550

Mann et al. 2004, Space Sci. Rev., 110, 269

Marsch, E., Pilipp, W. G., Thieme, K. M., Rosenbauer, H., et al. 1989, J. Geophys. Res., 94, 6893

Marsch, E. et al. 2002, Adv. Space Res., 29, 2027

Minato, T., Köhler, M., Kimura, H., Mann, I., Yamamoto, T. 2004, Astron. Astrophys., 424, L13

Möbius, E. et al. 2000, Adv. Space Res., 25, 196

Pellinen-Wannberg, A. et al. 2004, Geophys. Res. Letters, 31, L03812

Phaneuf, R. A., Janev, R. K., Pindzola, M. F. (Eds.) 1987: Atomic Data for Fusion. Vol. 5: Collisions of Carbon and Oxygen Ions with H, H2 and He, ORNL-6090 Oak Ridge National Laboratory Report

Schwadron, N. A. et al. 2000, J. Geophys. Res., 105, 7465

Sheeley Jr., N. R. et al. 1997, ApJ, 484, 472

Shull, J. M., van Steenberg, M. 1982, ApJS, 48, 95

Tielens, A. G. G. M., McKee, C. F., Seab, C. G., Hollenbach, D. J. 1994, ApJ, 431, 321

Tsurutani, B. T. et al. 2004, Icarus, 167, 89

Verner, D. A., Ferland, G. J., Korista, K. T., Yakovlev, D. G., 1996 ApJ, 465, 487

Wimmer-Schweingruber, R. & Bochsler, P., 2003 Geophys. Res. Lett., 30, 49-1

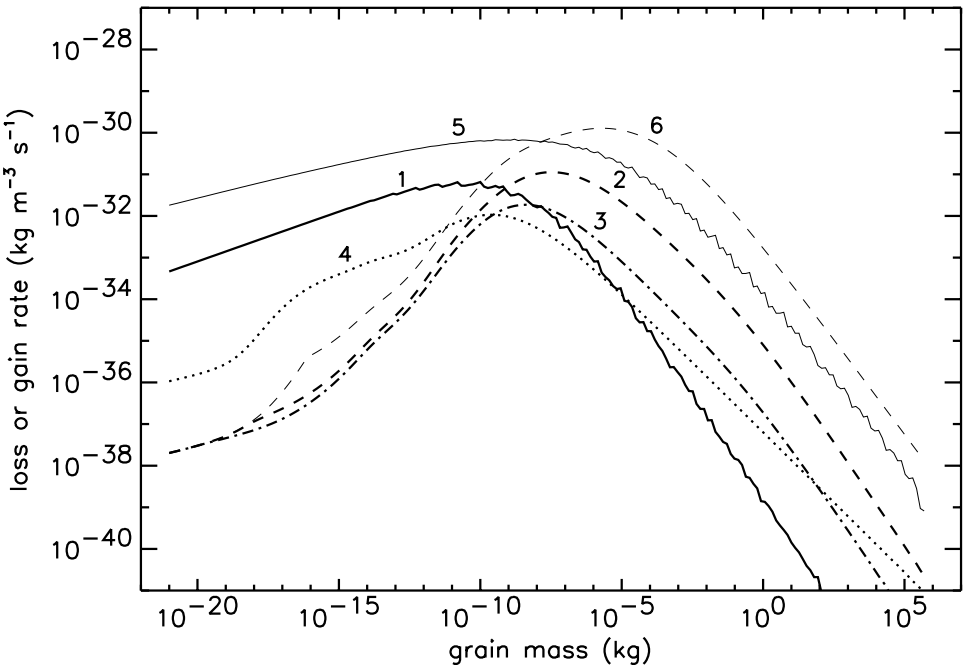

Fig. 1.— Calculated mass production rate (1), mass loss (fragmentation+vaporization) rate (2), mass vaporization rate (3) and Poynting-Robertson mass loss rate (4) at 0.3 AU for the model (A). The results corresponding to the collision model of Grün et al. (1985): the mass production rate (5) and mass loss rate (6) are shown for comparison. For the same dust distribution, our model gives smaller amount of fragmented material.

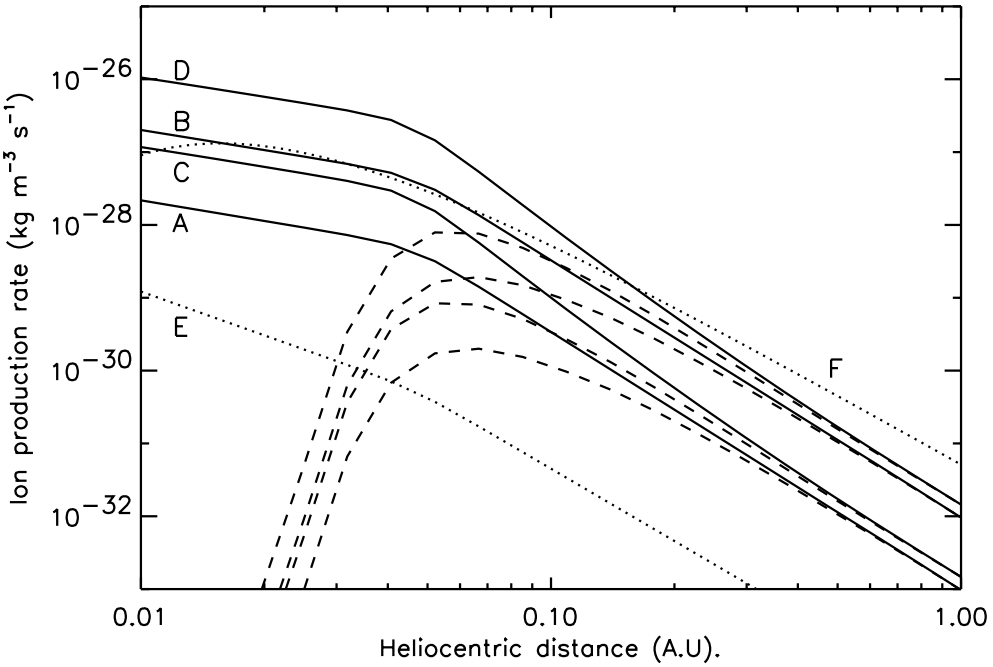

Fig. 2.— Calculated production rate of oxygen ions from collisional vaporization of silicate dust grains shown as a function of distance from the Sun, for the models (A), (B), (C) and (D) (curves A, B, C and D, respectively). The solid lines correspond to all charge states. The dashed lines show the effective sources of singly-charged ions (the source distributions folded with the probability that the ion arrives at 1 AU singly-charged). Dotted lines show the source distributions corresponding to production of oxygen pick-up ions (all charge states) by the solar wind surface interaction, for the case of the interplanetary flux model (denoted as E) and (denoted as F) for the dust density distribution assumed by Schwadron et al. (2000).

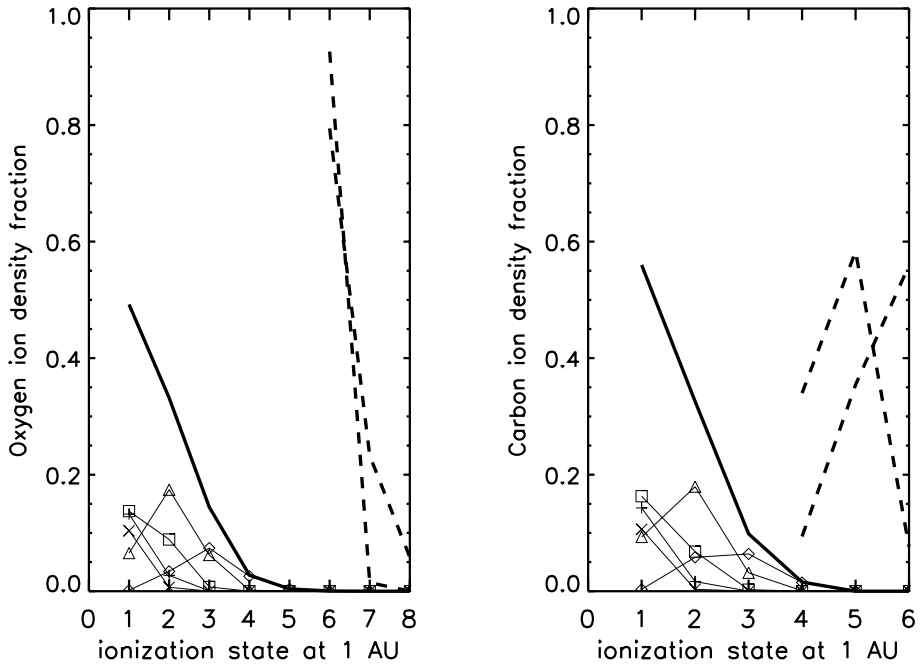

Fig. 3.— Calculated charge state distributions at 1 AU of oxygen and carbon ions produced by collisional vaporization of dust inward from 1 AU (solid lines). Contributions from the ions originating in different zones around the Sun are shown by symbols linked by thin lines. Rhombs, triangles, squares, plus signs and x signs denote the ions released in the regions 0.02 AU- 0.04 AU, 0.04 AU - 0.08 AU, 0.08 AU - 0.16 AU, 0.16 AU - 0.32 AU, and 0.32 AU - 0.64 AU, respectively. Note that the ions produced at short distances from the Sun arrive at 1 AU in high charge states. Sample charge state distributions in the bulk solar wind are shown for comparison (dashed lines).

Table 1: Results from model calculations.

Grain material[a]	Model	Mass supply required[b] (kg/s)	Mass vaporized[c] (kg/s)	β-meteoroids production[d] (kg/s)
silicate	(A)	$9.1\ 10^2$	$1.7\ 10^2$	$5.4\ 10^1$
silicate	(B)	$8.3\ 10^3$	$1.7\ 10^3$	$5.2\ 10^2$
silicate	(C)	$4.6\ 10^3$	$9.2\ 10^2$	$2.4\ 10^2$
silicate	(D)	$3.9\ 10^4$	$9.2\ 10^3$	$2.2\ 10^3$
carbon	(A)	$1.8\ 10^3$	$1.7\ 10^2$	$1.3\ 10^2$
carbon	(B)	$1.5\ 10^4$	$1.6\ 10^3$	$1.2\ 10^3$
carbon	(C)	$8.8\ 10^3$	$9.0\ 10^2$	$5.7\ 10^2$
carbon	(D)	$7.1\ 10^4$	$8.5\ 10^3$	$5.1\ 10^3$
ice	(A)	$1.5\ 10^3$	$8.3\ 10^2$	$3.5\ 10^1$
ice	(B)	$1.3\ 10^4$	$7.4\ 10^3$	$2.9\ 10^2$
ice	(C)	$7.3\ 10^3$	$4.3\ 10^3$	$1.5\ 10^2$
ice	(D)	$6.0\ 10^4$	$3.6\ 10^4$	$1.1\ 10^3$

[a]In model calculations the efficiencies of fragmentation and vaporization are assumed to be those of the materials indicated.

[b]Mass supply required to maintain the dust cloud inside 1 AU.

[c]Total mass of dust vaporized by collisions within 1 AU.

[d]Estimated as the net mass gain in the range 10^{18} to 10^{-15} kg: Mann et al. (2004).